Compensation Method Applied to Coriolis Mass Flow Metering

F. Koschmieder and H. Röck
Christian-Albrechts-University of Kiel
Kaiserstr. 2, 24143 Kiel, Germany
Tel: +49 431 880-6286, E-Mail: fk@tf.uni-kiel.de

Abstract: Coriolis mass flow meters (CMFM) are characterized by high accuracy and the ability to measure density and mass flow simultaneously. The sensitivity and zero point of the CMFM may change due to temperature gradients along the measuring pipe or mounting conditions. These changes have to be detected and corrected in order to assure high accuracy. A model based approach to estimate the zero point during normal operation and one-phase flow is presented. The approach exploits two characteristics of the measuring device: firstly the impact of mass flow upon the oscillation in the 2nd mode when the 1st mode is stimulated i.e. the operation principle of nearly all Coriolis mass flow meters and secondly the impact of mass flow upon the oscillation in the 1st mode when the 2nd mode is stimulated. Both of these characteristics are realized by compensation of Coriolis forces using MIMO-Phasor-Control.

Keyword: Coriolis, mass flow, sensitivity, zero point, phasor control

1. Introduction

The CMFM consists of a single straight measuring pipe with two sensors and actuators located symmetrically to the middle of the pipe (fig. 1). During normal operation, the 1st eigenmode (drive mode) is stimulated by two harmonic forces $\underline{F}_a$ and $\underline{F}_b$ operating in common mode. Without mass flow $\dot{m}$ the measured velocity signals $\underline{V}_a$ and $\underline{V}_b$ are in phase. Due to mass flow $\dot{m} > 0$, Coriolis forces with opposite directions in the in- and outlet of the pipe are induced and stimulate a further oscillation of the pipe in the 2nd eigenmode (Coriolis mode).

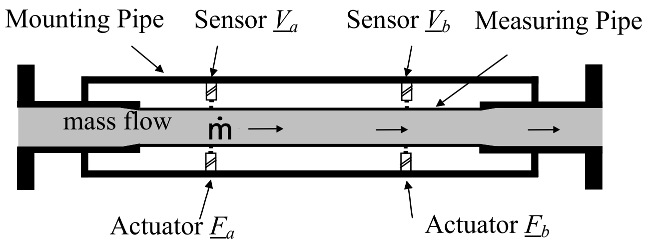

Fig. 1 Design of the CMFM

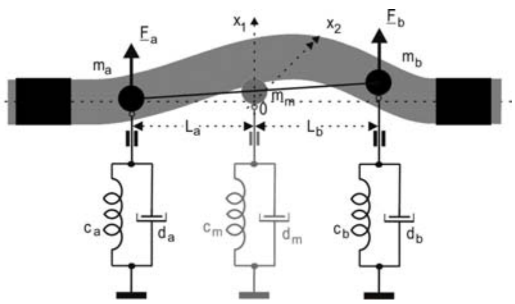

Fig. 2 Lumped parameter model

The superposition of both oscillations leads to a phase shift in the sensor signals $\underline{V}_a$ and $\underline{V}_b$ which is proportional to mass flow $\dot{m}$. With two actuators the CMFM can be stimulated either in its 1st or in its 2nd mode and thus allows for switching between different modes of operation necessary for detecting changes in sensitivity and zero point.

2. Mathematical model of the CMFM

Fig. 2 shows the lumped parameter model of the CMFM. The corresponding block-diagram is depicted in fig. 3. The forces $\underline{F}_a$ and $\underline{F}_b$ acting in common mode stimulate the pipe in its 1st eigenmode while push pull stimulation will result in an oscillation in 2nd mode. Using the driving

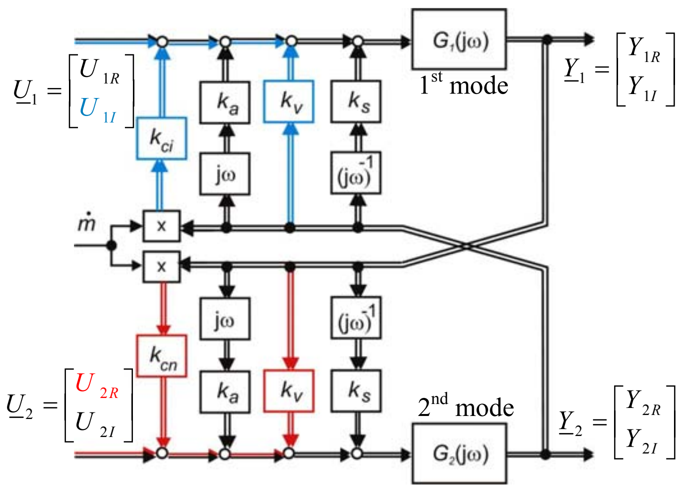

$\underline{U}_1 = \begin{bmatrix} U_{1R} \\ U_{1I} \end{bmatrix}$, $\underline{U}_2 = \begin{bmatrix} U_{2R} \\ U_{2I} \end{bmatrix}$, $\underline{Y}_1 = \begin{bmatrix} Y_{1R} \\ Y_{1I} \end{bmatrix}$, $\underline{Y}_2 = \begin{bmatrix} Y_{2R} \\ Y_{2I} \end{bmatrix}$

transfer functions of the i^th eigenmode:

$$G_i(j\omega) = \frac{k_i}{s^2 + 2d_i\omega_{0i}s + \omega_{0i}^2} \quad i = 1,2$$

$$d_i \ll 1,\ \omega_{01} < \omega_{02}$$

couplings:

acceleration-coupling: $k_a = m_b - m_a$

displacement-coupling: $k_s = c_b - c_a$

velocity-coupling: $k_v = d_b - d_a$

couplings caused by mass flow: k_{cn}, k_{ci}

— compensation of Coriolis forces by U_{1I} during operating mode *c*

— compensation of Coriolis forces by U_{2R} during operating mode *b*

Fig. 3 Block-diagram of the CMFM

signals $\underline{U}_1=(\underline{F}_a+\underline{F}_b)/2$ and $\underline{U}_2=(\underline{F}_a-\underline{F}_b)/2$ as inputs to the transfer functions $G_1(j\omega)$ and $G_2(j\omega)$ the oscillation in 1st and 2nd mode can directly be addressed.

Outputs of the model are the velocity signals $\underline{Y}_1=(\underline{V}_a+\underline{V}_b)/2$ and $\underline{Y}_2=(\underline{V}_a-\underline{V}_b)/2$ corresponding to the 1st and 2nd mode of oscillation as the electrodynamic sensors in the in- and outlet of the pipe measure velocities rather than displacements. Both of the modes of oscillation are coupled by mass flow $\dot{m}$ and additionally coupled due to asymmetries in the mechanical assembly and asymmetries in material properties, e.g. in Young's modulus [6]. These couplings are represented by the factors k_a, k_v and k_s. The couplings k_{cn} and k_{ci} are caused by mass flow represent the distributed Coriolis forces along the measuring pipe. They are regarded as being constant at single phase flow and only dependent on geometric properties. These parameters are estimated in a calibration procedure at factory's site. According to fig. 3 the velocity coupling k_v due to asymmetries in damping or mounting conditions is in parallel to the coupling constants k_{cn} and k_{ci} and therefore undistinguishable from mass flow. The analysis shows, that k_v represents the zero point of the meter.

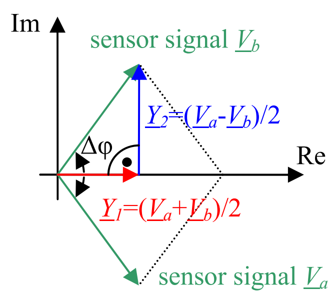

Fig. 4 Phasor diagram of the sensor signals

3. Measuring of the characteristics sensitivity and zero point

For a good signal to noise ratio, the CMFM is stimulated in its 1st eigenfrequency ω_{01} by nonlinear MIMO-Control together with phase control (fig. 5) which guarantees a stable oscillation of the measuring pipe in its 1st eigenfrequency [1]. This scheme provides simultaneous amplitude and phase control and thus allows for switching between the modes *a-c* of operation in tab. 1 and for estimating unknown coupling factors in the model. Commercial CMFM measure mass flow via the phase shift $\Delta\varphi(\dot{m}) = \measuredangle\underline{V}_a - \measuredangle\underline{V}_b$ between the sinusoidal sensor signals $\underline{V}_a$ and $\underline{V}_b$. If the phasors $\underline{Y}_1$ and $\underline{Y}_2$ are orthogonalised by control (fig. 4), the imaginary part Y_{2I} of phasor $\underline{Y}_2$ is directly proportional to mass flow $\dot{m}$ (mode of operation *a*). Accordingly the characteristics of the CMFM can be expressed in parameters of the model [6] as

$$y_n(\dot{m}) = \frac{\Delta\varphi}{2} = \frac{Y_{2I}}{Y_{1R}} = \underbrace{G_{2I}\,k_{cn}}_{\text{sensitivity}}\ \dot{m} + \underbrace{G_{2I}\,k_v}_{\text{zero point}} \quad (1)$$

Tab. 1 Operating modes of the CMFM for estimating sensitivity and zero point

operating modes	set points of the MIMO-Controller				characteristics of the CMFM
a	$Y_{1R}=W_{1R}$	$Y_{1I}=0$	$Y_{2R}=0$	uncontrolled $Y_{2I}\sim\dot{m}$	$y_n(\dot{m})=\frac{Y_{2I}}{Y_{1R}}=\underbrace{G_{2I}k_{cn}}_{\text{sensitivity}}\dot{m}+\underbrace{G_{2I}k_v}_{\text{zero point}}$
b	$Y_{1R}=W_{1R}$	$Y_{1I}=0$	$Y_{2R}=0$	$Y_{2I}=0$	$y_{comp}(\dot{m})=\frac{-U_{2R}}{Y_{1R}}=k_{cn}\dot{m}+k_v$
c	$Y_{1R}=0$	$Y_{1I}=0$	$Y_{2R}=0$	$Y_{2I}=W_{2I}$	$y_{inverse}(\dot{m})=\frac{-U_{1I}}{Y_{2I}}=k_{ci}\dot{m}+k_v$

As damping of the oscillation in 2nd mode is very small and the excitation frequency $\omega_B=\omega_{01}$ is far below its eigenfrequency ($\omega_{01}<<\omega_{02}$) the transfer function G_2 can be approximated by its imaginary part. Changes in temperature have an impact on materials properties and will change Young's Modulus and thus the transfer function G_2 . To estimate the imaginary part of G_2 an additional stimulus $U_{2R}=\Delta U_{2R}$ is injected to exite the 2nd mode and results in a variation of $\underline{Y}_2=Y_{2I}+\Delta Y_{2I}$. The stimulus $U_{2R}=\Delta U_{2R}$ can be interpretated as a virtual change in mass flow and thus allows for estimating G_{2I} [4] by:

$$G_{2I}=\frac{\Delta Y_{2I}}{\Delta U_{2R}} \qquad (2)$$

In the block diagram fig. 3 the outputs $\underline{Y}_1$ and $\underline{Y}_2$ are fed back to the inputs $\underline{U}_1$ and $\underline{U}_2$ via the velocity coupling k_v in parallel to the coupling constants k_{cn} and k_{ci}. Due to the symmetry of the lumped parameter model, the mass flow (couplings k_{cn} and k_{ci}) has an impact on both of the oscillations in 2nd and 1st mode. Exploiting this feature finally results in two characteristics of the meter for measuring mass flow.

The 1st characteristics will be obtained if the measurement of mass flow is mapped from the output Y_{2I} onto U_{2R} by compensating the oscillation of the 2nd mode. This can be done if the set point of the phasor controller is chosen as $Y_{2I}=0$ (operating mode *b*). The control action results in

$$U_{2R}=-(k_{cn}\dot{m}+k_v)Y_{1R} \qquad (3)$$

and the characteristics of the CMFM reads

$$y_{comp}(\dot{m})=\frac{-U_{2R}}{Y_{1R}}=k_{cn}\dot{m}+k_v \qquad (4)$$

In an analoguous way we derive the 2nd characteristics called the inverse characteristics by

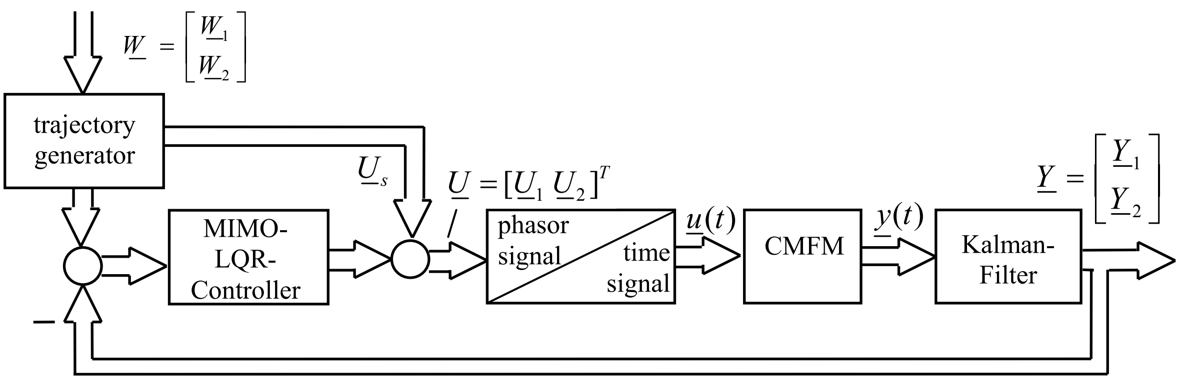

Fig. 5 Flatness based control-scheme for the phasor control of the CMFM

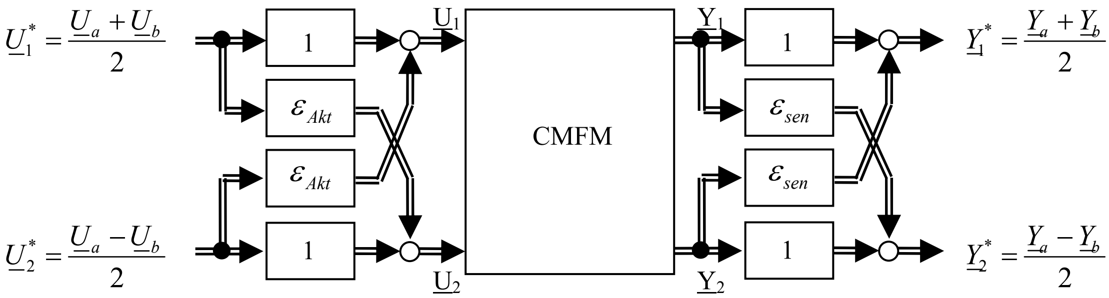

Fig. 6 Block-diagram of the CMFM with sensor and actuator couplings

mapping the output Y_{1I} onto U_{1I} and thus compensating the induced oscillation of the 1st mode. In this regime of operation only the oscillation in 2st mode is stimulated. The set points of the controller have to be changed accordingly i.e. $\underline{Y}_I=\underline{0}$ and $Y_{2I}=W_{2I}$ (operating mode *c*). The control action

$$U_{1I} = -(k_{ci}\dot{m} + k_v)Y_{2I} \qquad (5)$$

compensates the coupling from 2nd to 1st mode and U_{1I} represents mass flow. Finally, the invese characteristics of the meter reads

$$y_{inverse}(\dot{m}) = \frac{-U_{1I}}{Y_{2I}} = k_{ci}\dot{m} + k_v \qquad (6)$$

In the lumped parameter model the characteristics $y_{inverse}$ and y_{comp} should have in common the same zero point and therefore should allow for estimating the zero point during operation of the meter by exploiting both characteristics. The disadvantage of this approach however, i.e. switching between different modes of operation, can be solved by separating the measurements in frequency domain, e.g. the measurement of mass flow using the inverse characteristics should be done at a different frequency ω_{B2} with $\omega_{01} < \omega_{B2} < \omega_{02}$.

4. Fitting the characteristics by introducing sensor and actuator couplings

In practice there is a significant difference in the zero point of the characteristics $y_{inverse}$ and y_{comp} (cp. figs 7b and 7c). In order to fit the lumped parameter model to the measured characteristics, we introduce two further couplings called sensor and actuator coupling. These couplings can be interpreted as differences in actuator and sensor gain. A difference in actuator gain will always stimulate the 2nd mode of oscillation, as symmetric common mode stimulation is no longer possible with identical amplitudes of the harmonic drive signals $\underline{F}_a$ and $\underline{F}_b$.

In fig. 6 the block-diagram of the CMFM is extended by introducing sensor and actuator coupling. The actuating forces $\underline{F}_a$ and $\underline{F}_b$ are proportional to the input voltages $\underline{U}_a$ and $\underline{U}_b$ of the U/I-converter in fig. 8. The input $\underline{U}_1^*$ of the extended model represents the common mode stimulation while the push pull part is represented by $\underline{U}_2^*$.

$$\underline{U}_1 = \underline{U}_1^* + \varepsilon_{Akt}\underline{U}_2^* \qquad (7a)$$

$$\underline{U}_2 = \underline{U}_2^* + \varepsilon_{Akt}\underline{U}_1^* \qquad (7b)$$

where ε_{Akt} is introduced as actuator coupling. In an analogous way the new outputs

$$\underline{Y}_1^* = \underline{Y}_1 + \varepsilon_{Sen}\underline{Y}_2 \qquad (8a)$$

$$\underline{Y}_2^* = \underline{Y}_2 + \varepsilon_{Sen}\underline{Y}_1 \qquad (8b)$$

are introduced with ε_{Sen} as sensor coupling.

In an analogous way to the measurement of the characteristics y_{comp} in mode *b* without sensor and actuator coupling the set points for the controller are chosen as $\underline{Y}_1^* = [W_{1R}\ 0]^T$ and $\underline{Y}_2^* = \underline{0}$. Taking into account sensor and actuator coupling we get

$$U_{2R} = U_{1R}^* \varepsilon_{Akt} + U_{2R}^* \qquad (9a)$$

and

$$Y_{1R} = \frac{Y_{1R}^*}{1-\varepsilon_{Sen}^2} \qquad (9b)$$

Replacing Y_{1R} and U_{2R} in the characteristics y_{comp} leads to

$$\frac{-U_{2R}}{Y_{1R}} = \frac{-U_{1R}^* \varepsilon_{Akt} - U_{2R}^*}{\frac{Y_{1R}^*}{1-\varepsilon_{Sen}^2}} = k_{cn}\dot{m} + k_v \qquad (10)$$

or

$$y_{comp}^* = \frac{-U_{2R}^*}{Y_{1R}^*} = \underbrace{\frac{k_{cn}}{1-\varepsilon_{Sen}^2}}_{\text{sensitivity}}\ \dot{m} + \underbrace{\frac{1}{1-\varepsilon_{Sen}^2} k_v + \varepsilon_{Akt} \frac{U_{1R}^*}{Y_{1R}^*}}_{\text{zero point}} \qquad (11)$$

Compared to y_{comp} there is a difference in sensitivity and zero point in the new characteristics y_{comp}^*.
Calculating the inverse characteristic with sensor and actuator coupling results in

$$y_{inverse}^* = \frac{-U_{1I}^*}{Y_{2I}^*} = \underbrace{\frac{k_{ci}}{1-\varepsilon_{Sen}^2}}_{\text{sensitivity}}\ \dot{m} + \underbrace{\frac{1}{1-\varepsilon_{Sen}^2} k_v + \varepsilon_{Akt} \frac{U_{2I}^*}{Y_{2I}^*}}_{\text{zero point}} \qquad (12)$$

In both characteristics the sensitvity of the meter is smaller by a factor of $1/(1-\varepsilon_{Sen}^2)$ but the main difference in the characteristics is the zero point of y_{comp}^* and $y_{inverse}^*$. From the fact that there should be corresponding zero points in both of the characteristics we can calculate the actuator coupling by using $y_{comp}^*(\dot{m}=0)$ and $y_{inverse}^*(\dot{m}=0)$.

5. Practical Results

Measurements of the characteristics are shown in the diagrams 7a - 7c, corresponding to the deflection method (7a) and the two compensation methods (7b, c).
As in the deflection method the characteristics is

$$y_n = \frac{Y_{2I}}{Y_{1R}} = \frac{Y_{2I}^*}{Y_{1R}^*} = G_{2I}\ k_{cn}\ \dot{m} + G_{2I}\ k_v \qquad (13)$$

we get the sensitivity $k_{cn} = 5.304 \cdot 10^{-2}\ \frac{\text{min}}{\text{kg}}$ with $G_{2I} = 3.935 \cdot 10^{-3}$ and the zero point as $k_v = 9.36 \cdot 10^{-2}$.
The zero point in the deflection method is identical to the zero point in both of the compensation methods if the actuator coupling is appropriately chosen i.e. both of the characteristics y_{comp} and y_{invers} have identical zero points. Resulting from eqs. (11) and (12) the actuator coupling has to be chosen as

$$\varepsilon_{Akt} = \frac{y_{comp}^*(\dot{m}=0) - y_{inverse}^*(\dot{m}=0)}{\frac{U_{1R}^*}{Y_{1R}^*} - \frac{U_{2R}^*}{Y_{2R}^*}} = -2.965 \cdot 10^{-3} \qquad (14)$$

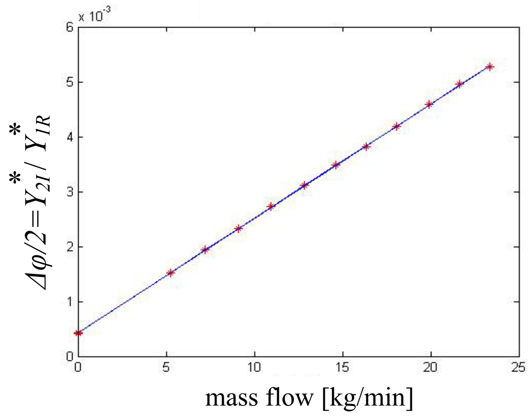

Fig. 7a Measured characteristic y_n

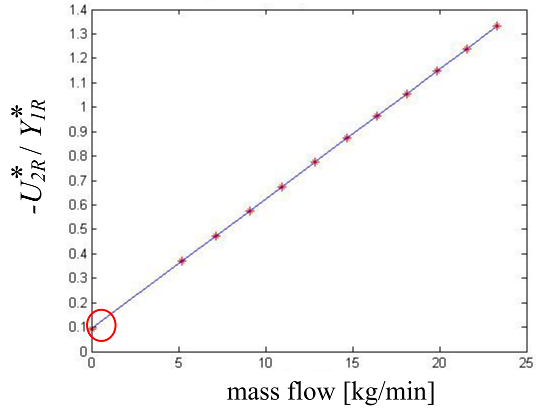

Fig. 7b Measured characteristic y^*_{comp}

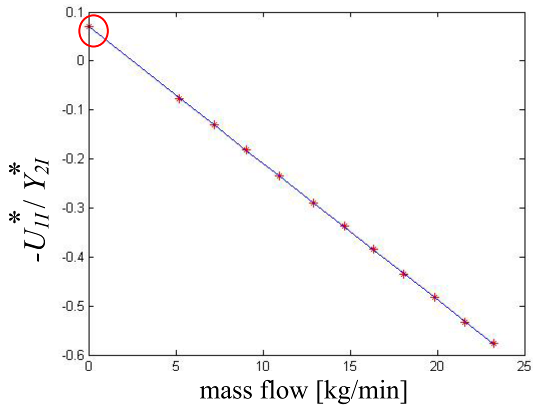

Fig. 7c Measured characteristic $y^*_{inverse}$

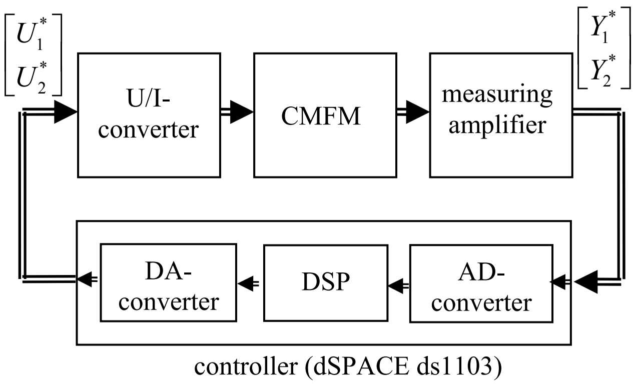

Fig. 8 Schematic of the control system

The parameter k_{cn} in the compensation method (mode of operation *b*) is in accordance with the sensitivity calculated via the deflection method, if G_{21} is calculated according to eq. (2). In the present design, the sensor coupling turned out to be rather small and is therefore neglected.

6. Conclusion

In this paper a model based control scheme has been presented allowing the CMFM to be operated in 3 different modes – (a) the deflection method and (b, c) two compensation methods.
The compensation of the Coriolis forces in the CMFM can be done in two different ways: (1) compensation of the 2nd mode oscillation when stimulating the meter in its 1st mode and (2) compensation of the 1st mode oscillation when stimulating the meter in its 2nd mode. To the best of our knowledge, the compensation method (2) has never been reported elsewhere. As the characteristics of both of the compensation methods differ in zero point, the lumped parameter model had to be modified by introducing sensor and actuator coupling that can be interpreted in terms of different actuator and sensor gains. If the actuator coupling is properly chosen, the zero point of the characteristics of both of the compensation methods and the characteristics of the deflection method are in good accordance. Exploiting the characteristics of both of the compensation methods, the zero point can be corrected either in a cyclic procedure or by separating the measurements in frequency domain.

References

[1] F. Koschmieder and H. Röck: *Advanced Phasor Control of a Coriolis Mass Flow Meter (CMFM)*. Proceedings of the XIX IMEKO World Congress, Vol. VI, pp. 1344-1349, Portugal, Lisbon, 6.-11. September 2009.

[2] J. Thomson, J. Dahl: *Phase shift effects for fluid conveying pipes with non-ideal supports*. Proceedings of XXII ICTAM, Adelaide, Australia, August 2009.

[3] H. Röck, T. Schröder, K. Kolahi and F. Koschmieder: *Flatness-Based Control of a Coriolis Mass Flowmeter*, ISMTII 2007, Sendai, Japan, 24.-27.9.2007.

[4] F. Koschmieder and H. Röck: *Bestimmung charakteristischer Größen eines CMD im laufenden Betrieb durch Anwendung der Zeigerregelung (Estimation of characteristic quantities of a CMFM by using a phasor control)*. GMA/ITG conference Sensors and Measurement Systems 2008, Tagungsband (VDI-Berichte) pp.265-272, Ludwigsburg, 11.-12. March 2008 (in German).

[5] R. Storm, K. Kolahi and H. Röck: *Model Based Correction of Coriolis Mass Flow meters*. 18th IEEE Instrumentation and Measurement Technology Conference, Vol. 2, pp. 1231-1236, Budapest, Hungary, 21.-23. May 2001.

[6] H. Röck and F. Koschmieder: *Model-Based Phasor Control of a Coriolis Mass Flow Meter (CMFM) for the Detection of Drift in Sensitivity and Zero Point*. Springer-Verlag, Recent Advances in Sensing Technology, Series: Lecture Notes in Electrical Engineering , Vol. 49, ISBN: 978-3-642-00577-0, 2009.